

The ionic character of the bonding in the Li tetrahedra is confirmed by the absence of electron density peaks in the Li—O bond directions. Fig. 5 shows two deformation electron density sections illustrating the Li—O bonds. One can clearly see 'lone-pair' regions of O(2)—O(5) atoms oriented towards the Li atom. This type of electron density distribution is quite common in an Li coordination polyhedron as reported, for example, by Shevryev *et al.* (1981) and Kirfel *et al.* (1983).

Concluding remarks

Our results provide refined parameters of the structure of LiB_3O_5 . Some Li—O and B—O distances differ from the results given by König & Hoppe (1978), by values which exceed the standard deviations by more than an order of magnitude. The presence of channels passing throughout the structure, parallel to c , and containing Li atoms suggests a possible ionic conductivity in this direction. Ionic conductivity in the directions perpendicular to c is hardly probable. All the B—O—B angles in the structures can be considered as close to 120° . One can then suppose that the electron deficiency in the B tetrahedra of the lithium triborate structure results in the formation of a delocalized orbital involving the entire boron—oxygen framework. This orbital can be roughly described as a sum of three-center orbitals forming the B—O—B bridges, the angle containing the O atom being equal to 120° . A similar situation has been reported previously by Shevryev *et al.* (1981) and Lipscomb (1973). The authors of an earlier work (Davydov, Derkacheva, Dunina, Zhabotinskii, Zolin, Koreneva & Samokhina, 1970)

assumed that the presence of delocalized multicentred valence orbitals accounts for the high nonlinear susceptibility in the crystals. It should also be noted that our results agree with the conclusions of the so-called theory of anionic groups for nonlinear-optical susceptibility in crystals (Chen & Liu, 1986). According to this theory, the larger the distortions in oxygen polyhedra or any other anionic groups of a structure, and the more inhomogeneous the electron deformation density distribution on the bonds in these groups, the higher are the values of the second-order microscopic susceptibility. As one can conclude from Chen, Wu & Li (1990), in the case of LBO the experimental data agree with the theoretical assumptions. Our structural data allow much more accurate calculations to be carried out in future work.

References

- CHEN, C. & LIU, G. (1986). *Annu. Rev. Mater. Sci.* **16**, 203–243.
 CHEN, C., WU, Y. & LI, R. (1990). *J. Cryst. Growth*, **99**, 790–798.
 DAVYDOV, B. L., DERKACHEVA, L. D., DUNINA, V. V., ZHABOTINSKII, M. E., ZOLIN, V. F., KORENEVA, L. G. & SAMOKHINA, M. A. (1970). *Pisma Zh. Eksp. Teor. Fiz.* **12**, 24–26.
 KIRFEL, A., WILL, G. & STEWART, R. F. (1983). *Acta Cryst.* **B39**, 175–185.
 KÖNIG, H. & HOPPE, R. (1978). *Z. Anorg. Allg. Chem.* **439**, 71–79.
 LIN, S., SUN, Z., WU, B. & CHEN, C. (1990). *J. Appl. Phys.* **67**, 634–638.
 LIPSCOMB, W. N. (1973). *Acc. Chem. Res.* **6**(8), 257–269.
 RADAEV, S. F., MURADYAN, L. A., MALAKHOVA, L. F., BURAK, YA. V. & SIMONOV, V. I. (1989). *Sov. Phys. Crystallogr.* **34**(6), 842–846.
 SHEVRYEV, A. A., MURADYAN, L. A., SIMONOV, V. I., EGOROV-TISMENKO, YU. K., SIMONOV, M. A. & BELOV, N. V. (1981). *Dokl. Akad. Nauk SSSR*, **257**(1), 111–114.
 ZUCKER, U. H., PERENTHALER, E., KUHS, W. F., BACHMAN, R. & SHULZ, H. (1983). *J. Appl. Cryst.* **16**(3), 358.

Acta Cryst. (1992). **B48**, 160–166

Phase Transition in Rubidium Nitrate at 346 K and Structure at 296, 372, 413 and 437 K

BY JUTTA POHL, DIETER POHL AND GUNADI ADIWIDJAJA

Mineralogisch-Petrographisches Institut der Universität Hamburg, Grindelallee 48, D-2000 Hamburg 13, Germany

(Received 22 May 1991; accepted 11 November 1991)

Abstract

Rubidium nitrate, RbNO_3 , $M_r = 147.474$, trigonal, space group $P3_1$ for both structures: below the irreversible first-order phase transition at 346 K and

above. Another crystal exhibited space group $P3_2$. Crystal growth from aqueous solution at 290 K. At 296 K: $a = 10.474$ (1), $c = 7.443$ (1) Å, $V = 707.2$ (2) Å³, $D_x = 3.116$ (1) g cm⁻³, refractive indices $n_\omega = 1.5250$ (1) and $n_e = 1.5267$ (3). After

heating (to 372 K) in a quartz capillary: $a = 10.506$ (3), $c = 7.469$ (3) Å, $V = 714.0$ (5) Å³, $D_x = 3.087$ (3) g cm⁻³, $F(000) = 612$, $\lambda(\text{Ag } K\alpha) = 0.56087$ Å, $\mu = 82.7$ cm⁻¹, $Z = 9$. Least-squares refinement with anisotropic temperature factors and an isotropic extinction parameter confirmed two different structures (before and after heating). Final $R = 0.0219$ (0.0301) for 970 (727) unique reflections with $I > 3\sigma(I)$. Both structures differ from that reported in the literature. The Rb atoms form a pseudocubic sublattice with nine pseudocubes per unit cell. Each NO₃ group is essentially parallel to one of the faces of its surrounding Rb-atom pseudocube. The phase transition is associated with a 90° flipping of one third of the NO₃ groups. On heating the crystal in a quartz capillary, a phase transition occurs between 296 and 372 K. The same crystal was used for measurements at 296, 372, 413, 437 and 296 K, respectively. Once formed, the new phase proved to be stable at all these temperatures. Differential thermal analysis revealed a transition temperature of 346 K.

Introduction

RbNO₃ is known to have four stable phases at atmospheric pressure. On heating, the room-temperature phase RbNO₃(IV) transforms to RbNO₃(III) at 437 K. This phase transition has been investigated by differential thermal analysis (Gordon & Campbell, 1955; Plyushev, Markina & Shklover, 1956), observations under the polarizing microscope, electrical conductance studies (Brown & McLaren, 1962), pyroelectric studies (Bury & McLaren, 1969), X-ray diffraction, dilatometric measurements (Salhotra, Subbarao & Venkateswarlu, 1968), infrared absorption spectroscopy (Karpov & Shultin, 1970), and ultraviolet absorption spectroscopy (Clever, Rhodes & Ubbelohde, 1963). Shamsuzzoha & Lucas (1982) (SL) solved the structure of RbNO₃(IV) by neutron diffraction. Dean, Hambley & Snow (1984) (DHS) recently confirmed this structure by X-ray diffraction single-crystal investigations. RbNO₃(III) is cubic and of the CsCl type with orientational disorder of the planar NO₃⁻ ions (Ahtee & Hewat, 1980; Shamsuzzoha & Lucas, 1987; Shinnaka & Yamamoto, 1981, 1983). The structure of RbNO₃(IV) at atmospheric pressure and with increasing temperature was initially studied in order to gain some insight into the mechanism of the phase transition at 437 K. For two reasons the information on this transformation remained limited. Firstly, as the crystal began to crack at 437 K it was impossible to study the transformation in single crystals. Secondly, we detected a hitherto unknown phase transition occurring between 296 and 372 K. The main results of the present study are a revised room-

temperature structure of RbNO₃(IV), a hitherto unknown phase transition at 346 K, and a new structure which has been detected at 372 K. A preliminary report of the phase transition has been given by Adiwidjaja, Brümmer & Pohl (1987).

Experimental, structure solution and refinement

Single crystals of RbNO₃ were grown by slow evaporation of an aqueous solution at 290 K. The *c*-axis needles had an approximately triangular cross-section. Two crystals were selected for data collection. One crystal (≤ 0.12 mm across and ≤ 0.27 mm long) was mounted on a glass fiber and used to determine an accurate structure at 296 K, which included the absolute configuration. The other crystal (≤ 0.29 mm across and ≤ 0.32 mm long), was mounted within a quartz-glass capillary and thereafter held at 373 K for 2 h in a drying-furnace. This crystal was then used to collect data at 296, 372, 413, 437 and 296 K. Unit-cell dimensions and integrated intensities were both measured on a CAD-4 diffractometer controlled by a PDP 11/34 computer under Enraf-Nonius (1983) software, and with a graphite monochromator [$\lambda(\text{Ag } K\alpha) = 0.56087$ Å] and high-temperature air-flow device (Tuinstra & Fraese Storm, 1978).

In order to calibrate this device two studies were performed in advance of data collection. Firstly, a thermocouple was brought into the air flow in place of the crystal. The temperature shown by the built-in thermometer of the air-flow device was ascertained to be proportional to the thermo-voltage in the range 296 to 473 K. Secondly, a calcite crystal was included in a quartz capillary in the same manner as the RbNO₃ crystal. The length of the *c* axis was determined as a function of temperature from a series of accurate measurements of the Bragg angles of 25 reflections at different temperatures between 296 and 353 K. These lengths were compared with the values given by Rao, Naidu & Murthy (1968). In this case the temperatures given by these authors were taken as being correct. The reading on the built-in thermometer then gave the temperature of the RbNO₃ crystal. At each temperature the unit-cell dimensions were determined from accurate measurements of the Bragg angles of 25 reflections with $10 < \theta < 20^\circ$. The results are listed in Table 1.

The integrated intensity of each reflection within a hemisphere of reciprocal space with $2 < \theta < 25^\circ$ and $-15 \leq h, k \leq 15, 0 \leq l \leq 11$ was measured from the smaller of the two crystals using an ω - 2θ -scan technique, for $\Delta\omega = (0.6 + 0.45\tan\theta)^\circ$. The maximum time measured was 300 s. Two standard reflections measured every 2 h showed no systematic variation of the intensities. Four other standard reflections measured every 300 reflections were used to control

Table 1. Lattice constants (\AA) of RbNO_3 as a function of temperature (K)

T	a	c
296 (0.1)	10.474 (1)	7.443 (1)
372 (3)	10.506 (3)	7.469 (2)
413 (5)	10.537 (4)	7.493 (3)
437 (9)	10.560 (6)	7.503 (5)
296 (0.1)*	10.455 (1)	7.421 (1)

* Values for the previously heated crystal.

the orientation. In order to determine the absolute configuration additional reflections with negative l were measured in the index range $-9 \leq h \leq 10$, $-10 \leq k \leq 2$, $-7 \leq l \leq 0$. A total of 6347 reflections included 2160 reflections which were considered to be unobserved: $I < 3\sigma_c(I)$, σ_c from counting statistics. The shape and dimensions of the crystal were used to calculate absorption corrections with maximum and minimum transmission values of 0.61 and 0.51, respectively. Lorentz and polarization corrections were made. Merging equivalent reflections [$R_{\text{int}}(F_{\text{obs}}) = 0.029$ for observed reflections and $R_{\text{int}}(F_{\text{obs}}) = 0.062$ for all reflections] resulted in 970 reflections which were used to solve and refine the structure.

The structure determined by DHS was refined using *SHELX76* (Sheldrick, 1975). Large shifts of some of the atomic coordinates and poor convergence of the least-squares refinement resulted. Following removal of one of the oxygen atoms [O(1)], difference Fourier synthesis gave a new position for this oxygen. On the basis of the modified structure further refinement with *ORXFLS3* (Busing *et al.*, 1971) was straightforward. The origin was fixed by the Rb(2) atom. Scattering factors for Rb, N and O, and anomalous-dispersion terms for all atoms, were taken from *International Tables for X-ray Crystallography* (1974, Vol. IV). In the final cycle all atoms were refined with anisotropic temperature factors and a secondary-extinction parameter ($q = 0.109 \times 10^4$) was included. The function minimized was $\sum w(|F_o| - |F_c|)^2$ where weights $w = 1/\sigma^2(F)$ were from counting statistics. Final agreement factors were $R = 0.0219$, $wR = 0.0204$ and $S = 1.491$. All shifts were less than 0.02σ . The maximum positive and negative features in the final difference electron density were $(\Delta\rho)_{\text{max}} = 0.46$, $(\Delta\rho)_{\text{min}} = -0.48 \text{ e \AA}^{-3}$. Large correlation coefficients occur between several parameters. It should be noted that there are pseudo-symmetries of a CsCl-type cubic structure whose positions are approximated by the Rb and N atoms.

The polar axis sense is 3_1 . This was affirmed in two ways. Firstly, for the space groups $P3_1$ and $P3_2$ the final wR values are 0.0204 and 0.0213, respectively. From Hamilton's test (Hamilton, 1965) $P3_2$ is

Table 2. Numbers of reflections, R values, final difference electron densities (e \AA^{-3}) and extinction parameters at different temperatures

	296 K	372 K	413 K	437 K	296 K*
Total No. of reflections	1530	1534	1542	1554	1527
Observed reflections	754	727	663	608	741
$R_{\text{int}}(F_{\text{obs}})$	0.037	0.028	0.030	0.045	0.038
$R_{\text{int}}(\text{all})$	0.047	0.042	0.052	0.073	0.050
R	0.0254	0.0301	0.0303	0.0384	0.0296
wR	0.0306	0.0354	0.0331	0.0415	0.0338
S	2.297	2.626	2.513	3.000	2.562
$(\Delta\rho)_{\text{max}}$	0.60	0.64	0.62	0.80	1.10
$(\Delta\rho)_{\text{min}}$	-0.50	-0.52	-0.50	-0.56	-0.44
$q \times 10^{-4}$	0.093	0.049	0.037	0.027	-

* Values for the previously heated crystal.

rejected on a significance level below 1%. Secondly, the data set included 22 Bijvoet pairs whose differences $|F_c(hkl)| - |F_c(\bar{h}\bar{k}l)|$ were greater than 2. These differences can be compared with those of the observed reflections. Only in three cases was the corresponding difference ΔF_o negative. Therefore, space group $P3_1$ is strongly supported again.

A quarter of reciprocal space with $2 \leq \theta \leq 20^\circ$ and $-12 \leq h, k \leq 12$, $0 \leq l \leq 9$ was measured at 296, 372, 413, 437 and 296 K for the larger crystal, enclosed in the capillary. With two exceptions the measurements were made as above. The scan width was $\Delta\omega = (0.7 + 45\tan\theta)^\circ$ and the crystal orientation was checked every 100 reflections. Lorentz, polarization and absorption corrections were applied with maximum and minimum transmission values of 0.24 and 0.21. The numbers of reflections measured, values of R_{int} from merging, values of R , wR and S from refinements as described above, maximum positive and negative difference electron densities, and isotropic extinction parameters are listed in Table 2.

Starting with the atomic positional coordinates of the smaller crystal, the 296 K structure refinement converged rapidly. Parameters refined, scattering factors, weighting scheme and programs used were as above. 34 Bijvoet pairs $hk0$ had differences $|F_c(hkl)| - |F_c(\bar{h}\bar{k}l)| \geq 1.28$. For all but one, the differences between the observed pairs were negative. Therefore, space group $P3_2$ is affirmed for this crystal. Nevertheless, space group $P3_1$ is used throughout this paper.

In solving the high-temperature structure at 372 K, the atomic positional coordinates of the room-temperature structure were used as a starting set. As refinement of one of the NO_3 groups was impossible, this group [around N(2)] was located from an electron density difference map. On the basis of the resulting positions the refinement converged rapidly. Likewise, these positions were used successfully to refine the structures measured at 413,

437 and 296 K. For the structures at 296 (before heating) and 372 K final atomic positional coordinates and equivalent isotropic thermal parameters are listed in Table 3.*

Refractive indices

Groth (1908) reported that rubidium nitrate is positive showing a weak birefringence with a very small angle between the optic axes. Approximate refractive indices were given as 1.51, 1.52 and 1.524. The Powder Diffraction File (JCPDS File No. 17-516) quotes $n_e = 1.526$, $n_o = 1.524$ and a slight biaxiality. The observed biaxiality is inconsistent with space group $P3_1$ or $P3_2$ as determined from X-ray diffraction. However, biaxiality can be simulated by submicroscopic domains (Rath & Pohl, 1971; Hauser & Wenk, 1976), even if the latter only occur in very small amounts. In order to clarify the character of the double refraction, an exact determination of the refractive indices was desirable. A microrefractometer spindle stage (Medenbach, 1985) was used to measure the refractive indices and to observe the biaxiality. The rubidium nitrate needles proved to be too long for use with the spindle stage. Several crystals were therefore cut perpendicular to the c axis. All of these cut crystals showed optical biaxiality with a very small angle between the optic axes. The crystals are positive and the acute bisectrix is near the needle axis. The axial angle varies from crystal to crystal. This is to be expected for crystals which are composed of differently oriented domains in varying fractions, whereas crystals of lowered symmetry would exhibit biaxiality with a fixed characteristic angle between the optic axes. It thus becomes quite clear that the cut crystals exhibit small amounts of twinning or domain building. It appears that single crystals of rubidium nitrate are uniaxial positive. The spindle-stage method gave refractive indices $n_e = 1.5267$ (3) and $n_o = 1.5250$ (1), based on the measurement of four crystals.

Crystal structures at 296 and 372 K

As shown above there are two structures: one grown from aqueous solution and the other found when the former was heated at 372 K in a capillary. A short description of both structures is given in the

* Lists of selected Bijvoet differences for both crystals, structure factors, anisotropic thermal parameters and deviations of N atoms from the plane of bonded oxygens for all data sets, and atomic positional coordinates and bond lengths and angles at 296, 413, 437 and 296 K (metastable form) have been deposited with the British Library Document Supply Centre as Supplementary Publication No. SUP 54705 (44 pp.). Copies may be obtained through The Technical Editor, International Union of Crystallography, 5 Abbey Square, Chester CH1 2HU, England.

Table 3. Fractional positional coordinates ($\times 10^4$) and B_{eq} values (\AA^2) for rubidium nitrate at 296 (upper line) and 372 K (lower line)

$$B_{eq} = \frac{4}{3} \sum_i \sum_j \beta_{ij} a_i \cdot a_j$$

	x	y	z	B_{eq}
Rb(1)	4474 (2)	5575 (2)	6483 (4)	2.5 (1)
	4373 (2)	5491 (2)	6900 (5)	2.9 (1)
Rb(2)	1231 (1)	2201 (1)	0	2.5 (1)
	1147 (2)	2241 (1)	0	3.3 (1)
Rb(3)	-2161 (1)	2299 (1)	6242 (1)	2.4 (1)
	-2107 (1)	2348 (1)	6485 (6)	3.0 (1)
N(1)	4612 (7)	5915 (7)	1628 (15)	2.4 (3)
	4400 (9)	5665 (12)	2169 (23)	2.3 (4)
N(2)	1009 (8)	2047 (8)	-4784 (15)	2.2 (3)
	1253 (11)	2035 (10)	-5191 (17)	2.5 (4)
N(3)	-2337 (9)	2260 (6)	959 (14)	1.7 (3)
	-2279 (10)	2331 (10)	1317 (29)	2.4 (4)
O(1)	4495 (7)	6778 (7)	2713 (8)	3.7 (2)
	4432 (9)	6649 (9)	3105 (16)	4.2 (3)
O(2)	3927 (8)	4597 (7)	1935 (10)	5.0 (3)
	3538 (11)	4373 (9)	2618 (21)	6.1 (4)
O(3)	5465 (7)	6419 (8)	389 (9)	4.0 (2)
	5172 (12)	6030 (15)	901 (15)	5.6 (5)
O(4)	22 (6)	1101 (6)	-3799 (9)	3.4 (2)
	1121 (11)	1076 (10)	-6178 (17)	5.5 (4)
O(5)	2310 (6)	2476 (7)	-4432 (10)	4.3 (2)
	2124 (11)	2314 (10)	-3889 (16)	5.2 (4)
O(6)	637 (7)	2519 (7)	-6081 (8)	3.9 (3)
	602 (14)	2673 (13)	-5341 (19)	6.9 (5)
O(7)	-2729 (9)	1458 (8)	2269 (9)	4.6 (9)
	-2674 (13)	1479 (11)	2541 (14)	5.2 (4)
O(8)	-1034 (6)	3091 (7)	553 (11)	4.4 (2)
	-1010 (9)	3200 (10)	942 (18)	5.6 (4)
O(9)	-3315 (6)	2246 (7)	-15 (8)	3.4 (2)
	-3306 (10)	2242 (9)	330 (18)	4.8 (4)

Abstract. The interatomic distances and angles are collected in Table 4.

The NO_3 groups are close to planar. Deviations of the nitrogen atom from the plane of the oxygens are within the margins of error (e.s.d.'s from refining one crystal plus discrepancies comparing both crystals).

Each Rb atom is enclosed by 12 oxygens. Eight shorter and four longer Rb—O bond lengths range from 2.96 to 3.16 \AA and from 3.26 to 3.71 \AA , respectively. The shorter bonds have average values of 3.06 (6) \AA at 296 K and 3.08 (5) \AA at 372 K, and the longer bonds 3.43 (10) and 3.45 (12) \AA .

The structures are comparable with each other and with the structure described by SL and DHS. As common features all three structures show Rb-atom pseudocubes, the nitrate groups being near a cube centre and essentially parallel to a pair of cube faces. With one exception each of the nitrate groups has one N—O bond almost parallel to a pseudocube cell edge. The exception concerns the crystal heated in a quartz capillary. Compared to the structure before heating two thirds of the NO_3 groups are unaltered. The group around the N(2) atom, however, is parallel to another pair of cube faces, and has one N—O bond [N(2)—O(6)] which is at an angle of only 4.6° to the diagonal of a pseudocube face. [This diagonal is given by the connection Rb(3)ⁱ to Rb(2)ⁱⁱ, where superscripts i and ii represent the equivalent posi-

Table 4. Interatomic distances (Å) and angles (°) at 296 (before heating) and 372 K

Standard deviations are in parentheses.

	296 K	372 K		296 K	372 K		296 K	372 K
Rb(1)—O(1)	3.072 (6)	3.073 (11)	Rb(2)—O(1)*	3.097 (6)	3.095 (8)	Rb(3)—O(2) ⁱⁱ	2.961 (6)	3.008 (10)
Rb(1)—O(1) ^v	3.131 (6)	3.107 (8)	Rb(2)—O(2)	3.043 (6)	3.086 (12)	Rb(3)—O(3) ⁱⁱⁱ	2.993 (5)	3.005 (10)
Rb(1)—O(1) ^{iv}	3.124 (7)	3.149 (10)	Rb(2)—O(3)*	3.391 (7)	3.407 (13)	Rb(3)—O(4) [†]	3.110 (6)	3.146 (10)
Rb(1)—O(2)	3.501 (8)	3.369 (14)	Rb(2)—O(4)*	3.078 (7)	3.100 (12)	Rb(3)—O(5) ⁱⁱⁱ	3.137 (6)	3.385 (12)
Rb(1)—O(2) ^v	3.662 (8)	3.471 (12)	Rb(2)—O(4) ⁱⁱ	3.082 (5)	3.147 (11)	Rb(3)—O(6) ^v	3.311 (7)	3.017 (11)
Rb(1)—O(3) ^v	3.068 (7)	3.078 (11)	Rb(2)—O(4) ^{iv}	3.104 (7)	3.123 (10)	Rb(3)—O(7)	3.059 (7)	3.053 (11)
Rb(1)—O(3) ^{iv}	3.286 (6)	3.434 (12)	Rb(2)—O(5)	3.452 (7)	3.069 (12)	Rb(3)—O(7) ⁱⁱⁱ	3.407 (8)	3.425 (10)
Rb(1)—O(5) ^v	2.963 (6)	3.030 (9)	Rb(2)—O(5) ^v	3.502 (7)	3.260 (10)	Rb(3)—O(8) ^v	3.376 (8)	3.490 (13)
Rb(1)—O(6) ⁱⁱⁱ	2.992 (6)	2.985 (11)	Rb(2)—O(6) ^v	3.026 (6)	3.592 (14)	Rb(3)—O(8) ⁱⁱⁱ	3.502 (7)	3.495 (12)
Rb(1)—O(7) ^{iv}	3.378 (8)	3.331 (12)	Rb(2)—O(6) ^{iv}	3.394 (6)	3.707 (13)	Rb(3)—O(9) ^v	3.026 (6)	3.115 (13)
Rb(1)—O(8) ^v	3.089 (7)	3.105 (10)	Rb(2)—O(7) ⁱⁱⁱ	2.968 (6)	3.016 (9)	Rb(3)—O(9) ⁱⁱⁱ	3.158 (6)	3.108 (12)
Rb(1)—O(9) ^{iv}	3.100 (6)	3.104 (9)	Rb(2)—O(8)	2.979 (6)	2.988 (10)	Rb(3)—O(9) ⁱⁱⁱ	3.075 (5)	3.115 (9)
N(1)—O(1)	1.26 (1)	1.24 (1)	N(2)—O(4)	1.25 (1)	1.20 (1)	N(3)—O(7)	1.22 (2)	1.20 (2)
N(1)—O(2)	1.22 (1)	1.24 (2)	N(2)—O(5)	1.24 (1)	1.27 (2)	N(3)—O(8)	1.23 (1)	1.21 (1)
N(1)—O(3)	1.21 (1)	1.18 (2)	N(2)—O(6)	1.23 (1)	1.18 (2)	N(3)—O(9)	1.25 (1)	1.27 (2)
O(1)—N(1)—O(2)	119 (1)	117 (2)	O(4)—N(2)—O(5)	119 (1)	116 (1)	O(7)—N(3)—O(8)	124 (1)	125 (2)
O(1)—N(1)—O(3)	118 (1)	117 (1)	O(4)—N(2)—O(6)	118 (1)	124 (2)	O(7)—N(3)—O(9)	118 (1)	115 (1)
O(2)—N(1)—O(3)	123 (1)	125 (1)	O(5)—N(2)—O(6)	122 (1)	126 (1)	O(8)—N(3)—O(9)	119 (1)	120 (2)

Symmetry code: (i) $x, y, 1+z$; (ii) $-y, x-y, \frac{1}{2}+z$; (iii) $-y, 1+x-y, \frac{1}{2}+z$; (iv) $-y, x-y, \frac{3}{2}+z$; (v) $1-y, 1+x-y, \frac{1}{2}+z$; (vi) $1-y, 1+x-y, \frac{3}{2}+z$; (vii) $-1+y-x, -x, \frac{1}{2}+z$; (viii) $y-x, -x, -\frac{1}{2}+z$; (ix) $y-x, -x, \frac{1}{2}+z$; (x) $y-x, 1-x, -\frac{1}{2}+z$; (xi) $y-x, 1-x, \frac{1}{2}+z$.

* At 296 K there is no superscript, and at 372 K superscript (i).

† Superscripts are (i) and (iv) at 296 and 372 K, respectively.

tions $x, y, z-1$ and $y-x, -x, z-\frac{1}{2}$, respectively.] Therefore, on heating the crystal, a phase transition occurred. After cooling, the new structure proved to be metastable at room temperature. For both structures a view (*ORTEPII*; Johnson, 1976) of the nitrate ions in the asymmetric unit is illustrated in Fig. 1 of Adiwidjaja, Brümmer & Pohl (1987) and the arrangement of the nitrate groups around the 3_1 axes is shown in Fig. 1 of the present paper.

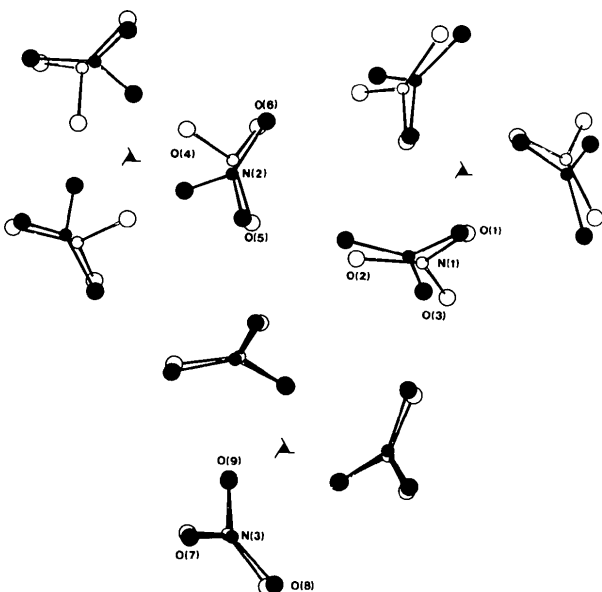


Fig. 1. Arrangement of the nitrate groups around the 3_1 axes in RbNO_3 at 296 (open circles) and 372 K (full circles) viewed along the c axis.

In discussing the RbNO_3 structures, the question arose as to whether the structure described by SL and DHS is a third phase that can exist at room temperature and atmospheric pressure. Therefore, the observed structure factors reported by these authors and deposited with the British Library Document Supply Centre, were refined using *ORXFLS3* (Busing *et al.*, 1971) and *SHELX76* (Sheldrick, 1975). In order to compare the results, all three structures were used as a starting set for the data of SL and DHS. The refinement converged each time. Several atomic parameters, however, were highly correlated. Moreover, bond lengths and angles within the nitrate groups deviated remarkably from regularity. Nevertheless, based on a discussion of the bonds none of the structures could be preferred. Comparison of the R values also gave no unambiguous decision. Therefore, it is concluded that the data of SL and DHS are too inaccurate to determine unambiguously the orientation of the nitrate groups.

Phase transitions up to 437 K

Phase III RbNO_3 (437 to 492 K) has a cubic CsCl structure, $Pm\bar{3}m$, with one molecule per unit cell. Accordingly, the rubidium atoms can be positioned at the corners of a cube centred on the nitrate group. In order to meet the symmetry requirements of space group $Pm\bar{3}m$, orientational disorder of the planar triangle-formed nitrate group is necessary. Ahtee & Hewat (1980), Shinnaka & Yamamoto (1981, 1983) and Shamsuzzoha & Lucas (1987) have put forward a 12-orientation model. In this model the plane of

the nitrate group is parallel to a pair of cube faces and one N—O bond is parallel to a cube edge, making 12 orientations altogether.

As compared with the orientationally disordered structure of phase III the structure at room temperature is completely ordered. Each nitrate group forms an approximately planar equilateral triangle located close to the centre of a pseudocube built up of the rubidium atoms. Within a pseudocube the orientation is the same as in the above 12-orientation model. So far this model is supported by the structure determination at room temperature. To make the orientational disorder also plausible two forms of motion of the rigid nitrate group have to be shown to exist at elevated temperatures. These motions are an in-plane rotation of the group and a flipping of its plane between different pairs of the surrounding cube faces. The first is well known as librational motion of planar molecules but is difficult to distinguish from discrete states of disorder as required for the phase transition at 437 K. However, our data do not allow this topic to be decided upon. The second motion was observed in connection with the phase transformation below 372 K, thus giving further support to the above 12-orientational model. One N—O bond, however, is almost diagonal to a face of the pseudocube. Incorporation of this orientation into the 12-orientational model is impossible.

The present study, based on structure determinations at different temperatures, revealed a phase transition between 296 and 372 K. The high-temperature form proved to be stable up to 437 K. After cooling, this structure was also determined at room temperature, and is hence metastable. Therefore, on heating a crystal of RbNO_3 in a capillary, an irreversible first-order phase transition took place. Before mounting on the diffractometer, the enclosed crystal was held at 373 K for 2 h but showed no phase transformation. It is therefore concluded that the transformation is very sluggish. As the phase transition is connected with a decrease in volume the possibility of a pressure-induced phase transformation arose, as an alternative to a temperature-induced transformation at atmospheric pressure, and was investigated.

In order to throw light on the above transition, two additional investigations were made. In the first, several single crystals were held at 383 K for 40 h. Two of these crystals were mounted on the diffractometer and used to measure the integrated intensities of 18 selected reflections showing remarkable differences in intensities for both structures. Analysis of the data revealed that one crystal underwent a phase transition, whereas the other still showed the room-temperature form. Therefore, the phase transition is not pressure induced but takes place at atmospheric pressure. The sluggishness of the

transformation is confirmed by the observation that only one crystal showed the high-temperature form.

In the second investigation, the differential thermal analysis (DTA) technique was employed. A Netzsch Simultan-Thermo-Analyse-429 apparatus, with Pt—Rh thermocouples and platinum pans, was used to measure the DTA curves of RbNO_3 powder of stated purity 99.9% from Johnson Matthey. Two facts limit the accuracy of the measurement. Firstly, the precise determination of temperature is impossible below 400 K with Pt—Rh thermocouples. Secondly, the small latent heat of transformation requires large amounts of RbNO_3 powder to be used to detect the phase transformation at all. These large amounts are known to give too high a transition temperature. A DTA curve of 385 mg RbNO_3 , measured against $\alpha\text{-Al}_2\text{O}_3$ with a heating rate of 5 K min^{-1} , is shown in Fig. 2. On heating, the peak at 359 K corresponds to the transition detected first in the present study, whereas the peaks at 449 and 520 K correspond to the well-known phase transitions at 437 and 492 K, respectively. On cooling, only two peaks are seen, at 487 and 423 K, corresponding to the latter phase transitions, whereas the first transition is undetectable because of an irreversible phase transformation. It can be shown that averaging of the values on heating and cooling normally gives values close to the transformation temperature (Schultze, 1969). This has been observed in the present investigation for the 437 K phase transition showing a mean value

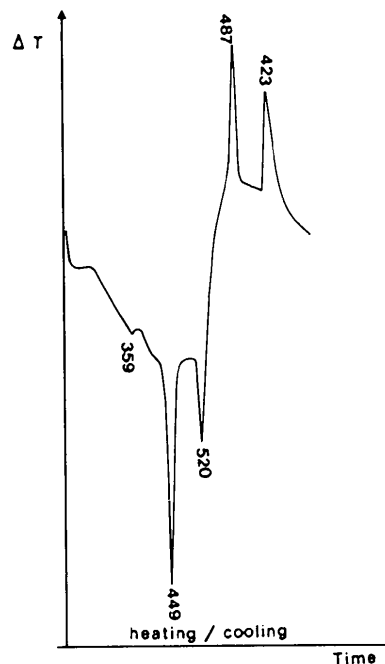


Fig. 2. DTA curve of RbNO_3 between room temperature and 513 K.

of 436 K. Therefore, the value measured on heating alone shows a difference of 13 K as compared with the corresponding mean value. If this misfit is transferred to the observed peak at 359 K, a corrected transition temperature of 346 (10) K results.

We thank Dr J. C. Eck for carrying out the thermal analyses.

References

- ADIWIDJAJA, G., BRÜMMER, J. & POHL, D. (1987). *Z. Kristallogr.* **178**, 3–4.
- AHTEE, M. & HEWAT, A. W. (1980). *Phys. Status Solidi*, **A58**, 525–531.
- BROWN, R. N. & MCLAREN, A. C. (1962). *Acta Cryst.* **15**, 974–976.
- BURY, P. C. & MCLAREN, A. C. (1969). *Phys. Status Solidi*, **31**, 799–806.
- BUSING, W. R., MARTIN, K. O., LEVY, H. O., ELISSON, R. D., HAMILTON, W. C., IBERS, J. J., JOHNSON, C. K. & THIESSEN, W. A. (1971). *ORXFLS3*. Oak Ridge National Laboratory, Tennessee, USA.
- CLEAVER, B., RHODES, E. & UBBELOHDE, A. R. (1963). *Proc. R. Soc. London Ser. A*, **276**, 453–460.
- DEAN, C., HAMBLEY, T. W. & SNOW, M. R. (1984). *Acta Cryst.* **C40**, 1512–1515.
- Enraf–Nonius (1983). *CAD-4 Operators Manual*. Enraf–Nonius, Delft, The Netherlands.
- GORDON, S. & CAMPBELL, C. (1955). *Anal. Chem.* **27**, 1102–1109.
- GROTH, P. (1908). *Chemische Kristallographie*, Vol II, p. 75. Leipzig: Verlag Wilhelm Engelmann.
- HAMILTON, W. C. (1965). *Acta Cryst.* **18**, 502–510.
- HAUSER, J. & WENK, H.-R. (1976). *Z. Kristallogr.* **143**, 188–219.
- JOHNSON, C. K. (1976). *ORTEP11*. Report ORNL-5138. Oak Ridge National Laboratory, Tennessee, USA.
- KARPOV, S. V. & SHULTIN, A. A. (1970). *Phys. Status Solidi*, **39**, 33–38.
- MEDENBACH, O. (1985). *Fortschr. Mineral.* **63**, 111–133.
- PLYUSCHEV, V. E., MARKINA, I. B. & SHKLOVER, L. P. (1956). *Dokl. Akad. Nauk SSR*, **108**, 645–647.
- RAO, K. V. K., NAIDU, S. V. N. & MURTHY, K. S. (1968). *J. Phys. Chem. Solids*, **29**, 245–248.
- RATH, R. & POHL, D. (1971). *Contrib. Mineral. Petrol.* **32**, 74–78.
- SALHOTRA, P. P., SUBBARAO, E. C. & VENKATESWARLU, P. (1968). *Phys. Status Solidi*, **29**, 859–864.
- SCHULTZE, D. (1969). *Differentialthermoanalyse*, p. 51. Weinheim: Verlag Chemie.
- SHAMSUZZOHA, M. & LUCAS, B. W. (1982). *Acta Cryst.* **B38**, 2353–2357.
- SHAMSUZZOHA, M. & LUCAS, B. W. (1987). *Acta Cryst.* **C43**, 385–388.
- SHELDRIK, G. M. (1975). *SHELX76*. Program for crystal structure determination. Univ. of Cambridge, England.
- SHINNAKA, Y. & YAMAMOTO, S. (1981). *J. Phys. Soc. Jpn*, **50**, 2091–2094.
- SHINNAKA, Y. & YAMAMOTO, S. (1983). *J. Phys. Soc. Jpn*, **52**, 3437–3440.
- TUINSTR, F. & FRAASE STORM, G. M. (1978). *J. Appl. Cryst.* **11**, 257–259.

Acta Cryst. (1992). **B48**, 166–172

Structural Instabilities of the Trigonal Coordinated Water Molecules in $\text{Ba}(\text{IO}_3)_2 \cdot \text{H}_2\text{O}$ and $\text{Pb}(\text{ClO}_3)_2 \cdot \text{H}_2\text{O}$ Studied by X-ray and Neutron Diffraction at 25 and 295 K

BY TH. KELLERSOHN AND H. D. LUTZ*

Anorganische Chemie I, Universität GH Siegen, Postfach 101240, D-5900 Siegen, Germany

TH. VOGT

Institut Laue–Langevin, BP 156X, F-38000 Grenoble CEDEX, France

AND R. G. DELAPLANE AND I. OLOVSSON

Inorganic Chemistry, Institute of Chemistry, Uppsala University, Box 531, S-75121 Uppsala, Sweden

(Received 1 October 1991; accepted 13 November 1991)

Abstract

Structural parameters are given for the isotopic title compounds, both monoclinic, $I2/c$, $Z = 4$. Barium diiodate monohydrate, $\text{Ba}(\text{IO}_3)_2 \cdot \text{H}_2\text{O}$: $M_r = 505.16$, $T_1 = 295$ K, neutron data, $R = 0.0359$ for 559 observed unique reflections; $T_2 = 25$ K, X-ray data, $R = 0.0291$ (2327 reflections). Lead dichlorate mono-

hydrate, $\text{Pb}(\text{ClO}_3)_2 \cdot \text{H}_2\text{O}$: $M_r = 392.11$, $T_1 = 295$ K, neutron data, $R = 0.0296$ (480 reflections) and 0.0351 (466 reflections) for two independent investigations on different crystals; $T_2 = 25$ K, neutron data, $R = 0.0302$ (755 reflections). An inter-experimental comparison indicates that the room-temperature neutron data for $\text{Pb}(\text{ClO}_3)_2 \cdot \text{H}_2\text{O}$ are largely free of systematic errors, notably extinction effects. At room temperature the water molecules in both compounds exhibit

* Author to whom correspondence should be addressed.